Journal of
Ceramic Science
and Technology

J. Ceram. Sci. Technol., **09** [3] 263-270 (2018)
DOI: 10.4416/JCST2018-00011
available online at: http://www.ceramic-science.com

Microstructure, Growth Kinetics and Formation Mechanism of Oxide Layers on AlN Ceramic Substrates

Ye Cao[1], Haixian Xu[2], Jun Zhan[2], Hao Zhang[2], Song Cui[2], Wenming Tang[*1]

[1]School of Materials Science and Engineering, Hefei University of Technology, Hefei 230009, China;
[2]43 Institute, China Electronics Technology Group Corporation, Hefei 230088, China

received February 8, 2018; received in revised form March 14, 2018; accepted April 17, 2018

Abstract

AlN ceramic substrates doped with 2 wt% Y_2O_3 were oxidized at temperatures ranging from 1000 °C to 1300 °C for various times in air. Microstructure, growth kinetics and formation mechanism of the oxide layers were studied. The results show that oxidation originates from the AlN grain boundaries and then extends into the AlN grains to form a core-shell structure composed of the unoxidized AlN core wrapped in the continuous nanocrystalline Al_2O_3 layer. A continuous pore network is distributed over the oxide layer and connected with the AlN reaction interface, which actually acts as the O_2/N_2 rapid diffusion path. As a result, oxidation of the AlN substrates follows reaction-rate-controlled kinetics. An activation energy of 260.5 kJ mol^{-1} of the oxidation process is then derived. Finally, a model involving the microstructure and mechanism of the oxide layer formation on the AlN substrates is established.

Keywords: AlN ceramic substrate, oxidation, microstructure, kinetics, formation mechanism

I. Introduction

With rapid development of power electronic technology, the chip integration level and power density of the microelectronic components and devices have been rapidly increased. Extra-high heat-dissipation ability of the components and devices is therefore required [1]. Direct-bonding copper (DBC) substrates have become the most important electronic circuit boards for multichip power semiconductor modules [2–4]. AlN ceramics have superior properties, i.e. the high TC (320 W m^{-1} K^{-1} in theory, 180–200 W m^{-1} K^{-1} for sintered polycrystalline ceramics) and the low CTE match the chip materials (AlN: 4.2×10^{-6} K^{-1}, Si and GaAs: 3–4×10^{-6} K^{-1}) [5, 6]. AlN-DBC substrates therefore have great potential in power semiconductor devices, for instance as insulated gate bipolar transistors (IGBT), as alternatives to Al_2O_3-DBC ones [7, 8]. To achieve strong adhesion of the thick Cu foil to the AlN ceramic substrate, the AlN ceramic substrate must first be oxidized to form an oxide layer measuring several microns in thickness [2, 9–12]. Oxidation of AlN is therefore an important topic in both science and technology.

Oxidation of polycrystalline AlN ceramics is complicated because the process is influenced by various factors [13–24]. Of these, the oxidation temperature and the sintering additives in the AlN ceramics are the two factors that are always emphasized. Osborne *et al.* [13] have reported that at temperatures ranging from 1150 °C to 1350 °C in air, oxidation of polycrystalline AlN substrates without any sintering additives is controlled by the interfacial reaction rate with an activation energy of 175 kJ mol^{-1}; while at temperatures ranging from 1350 °C to 1750 °C, oxidation behavior is controlled by the diffusion rate with a higher activation energy of 395 kJ mol^{-1}. Bellosi *et al.* [14] reported that the oxidation of pure AlN and 3-wt%-Y_2O_3-doped AlN substrates in air both followed interfacial-reaction-controlled kinetics. On the contrary, the oxidation mechanism of the 2-wt%-CaC_2-doped AlN substrates varies from the linear rate law (600–1200 °C) to the parabolic rate law (> 1250 °C). Yeh *et al.* [15] established a simple oxidation model of the 2-wt%-Y_2O_3-doped AlN substrates oxidized at 1050–1350 °C in air by means of direct measurement under a scanning electron microscope (SEM). In the model, the micropores are distributed in the oxide layer discontinuously, so the bulk diffusion of O_2 (or O^{2-}) in the oxide layer may be the rate-controlled step. On the other hand, although the oxidation mechanism is unchangeable, the oxidation kinetics of the AlN ceramics can be changed by the oxidation atmosphere. For example, the oxidation rate of the AlN ceramics increases with increasing humidity of the atmosphere [16–18].

As mentioned above, lots of research has concentrated on the oxidation of AlN ceramics, however, the key issue of the microstructure of the oxide layer and its effect on the oxidation behavior of AlN ceramics is still unclear. Moreover, the influence of Y_2O_3, the most commonly used sintering additive in polycrystalline AlN ceramics [25], has not been clarified. And hence, in-depth study on the oxidation of AlN ceramics is still required.

In this work, commercial AlN ceramic substrates doped with 2 wt% Y_2O_3 were chosen as the experimental materials. The AlN substrates were oxidized at 1000–1300 °C in air, following an industrial process. Surface morpholo-

* Corresponding author: wmtang69@126.com

gies, microstructures of the oxide layers and the oxidation kinetics of the AlN substrates were investigated. Finally, a model concerning the formation and growth of oxide layers on the AlN ceramic substrates was developed.

II. Experimental

Commercial 2-wt%-Y_2O_3-doped AlN substrates (Maruwa Co. Ltd., Japan) with a thickness of 0.635 mm and surface roughness (R_a) of 0.3 μm were laser-cut into square samples measuring 10 mm × 10 mm in size. The samples were oxidized in a KSL-1800X type chamber furnace at 1000, 1100, 1200 and 1300 °C in air for 50, 100, 150, 250 and 350 min, respectively. The heating rate was set to 5 K/min^{-1} from room temperature to 900 °C and then 8 K/min^{-1} from 900 °C to the set temperature. After holding, the samples were then cooled to 900 °C at a rate of 5 K/min^{-1} and finally cooled with the furnace.

A SU8020 field emission scanning electron microscopy (FE-SEM) equipped with an Oxford INCA type energy-dispersive spectrometer (EDS) was employed for multi-point measurement of the oxide layer. For each sample, five different positions were chosen randomly to obtain the average thickness of the oxide layer. Of course, the equipment was also used for surface morphology and cross-sectional fractograph observation and the local composition test. Phases of the AlN ceramic substrates before and after oxidation were analyzed in an X'Pert PRO MPD X-ray diffractometer (XRD) with CuKα radiation and the tube voltage and current of 40 kV and 40 mA, respectively. The scanning rate was set to 0.02° per 20 s and the scanning angle range (2θ) from 10° to 90°.

III. Results and Discussion

(1) Microstructure

The as-received AlN substrate is composed of AlN and a small amount of YAG ($Y_3Al_5O_{12}$) (Fig. 1a). After oxidation at 1000 °C, corundum-type α-Al_2O_3 was detected in the oxidized AlN substrate (Fig. 1b). The diffraction peak intensity of α-Al_2O_3/AlN increases/decreases with elevating oxidation temperature (Fig. 1b – d). The increment of α-Al_2O_3 indicates the increase in the thickness of the oxide layer. Finally, the oxide layer is thick enough to completely shield the AlN diffraction peaks in Fig. 1e, after the AlN substrate had oxidized at 1200 °C for 350 min.

As shown in Fig. 2, the AlN substrate is uniformly oxidized, having a clear, flat oxide layer/AlN interface. The N content of the oxide layer is very low, indicating that the previously present AlN grains have completely transformed into α-Al_2O_3 (Fig. 2d). The Y-rich spots (YAG in Fig. 1) are uniformly distributed in the AlN substrate and the oxide layer with identical size and distribution (Fig. 2e). Grains A and B in Fig. 3 were identified as the YAG grains by means of EDS analysis (55.7 wt% Y, 22.8 wt% O and 21.5 wt% Al). Grain A is situated at a triple AlN grain boundary, corresponding to the larger bright spot in Fig. 2e. Grain B is located preferentially at a binary AlN grain boundary, corresponding to the smaller dispersive bright point in Fig. 2e. The YAG grains play important roles in the oxidation of the AlN ceramic substrates, as described in the following.

The AlN grain is equiaxial and about 2 – 4 μm in size (Fig. 4a). After the AlN substrate oxidizes at 1000 °C, the chemical composition of the square area in Fig. 4b is 59.9 wt% Al, 39.7 wt% O and 0.4 wt% N, indicating that oxidation of the AlN substrate is taking place. The oxide layer is dense without any cracks (Fig. 4b). However, during oxidation at 1100 °C and above, high-density microcracks are generated along the Al_2O_3 grain boundaries, several large cracks finally form in the oxide layer of the AlN substrate oxidized at 1200 °C (Fig. 4c, d).

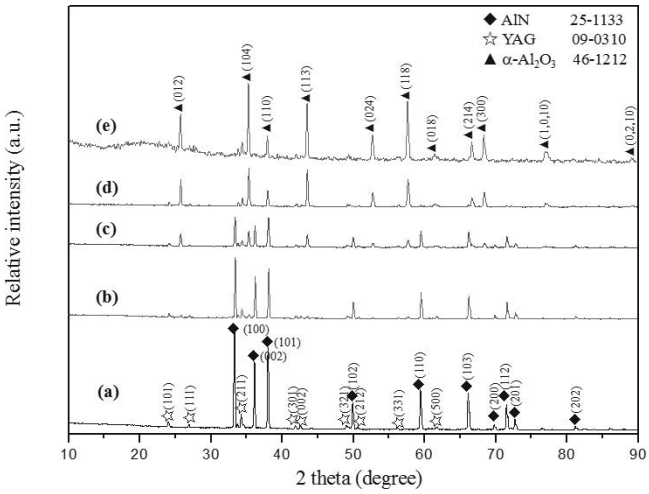

Fig. 1: XRD patterns of the AlN substrates (a) As-received and oxidized at different temperatures for 350 min (b) 1000 °C; (c) 1100 °C; (d) 1200 °C; (e) 1300 °C.

After the AlN substrate has oxidized at 1000 °C for 150 min, the oxide layer thickness is only 0.7 μm. It increases rapidly to 5.5 μm with elevation of the oxidation temperature to 1100 °C. These oxide layers are dense and bond tightly with the AlN substrates (Fig. 5a, b). The oxide layer increases to 42 μm and 220 μm after the AlN substrates have oxidized at 1200 °C and 1300 °C for the same time, respectively. As shown in Fig. 5c, longitudinal cracks perpendicular to the Al_2O_3/AlN interface and transverse cracks parallel to the interface coexist in the oxide layer.

(2) Growth kinetics

In Fig. 6, linear relationships of the thickness of the oxide layers versus the oxidation time are shown after the AlN substrates have oxidized at 1000 – 1300 °C, indicating reaction-rate-controlled kinetics. As shown in Figs. 2 and 3, the existence of the YAG grains results in broadening of the AlN grain boundaries, providing fast diffusion paths for O_2 in the unoxidized AlN substrates. Meantime, there are high-density continuous tubular pores along the Al_2O_3 grain boundaries in the oxide layers. The tubular pores act as a fast path for O_2 diffusion from the atmosphere to the Al_2O_3/AlN reaction interface. The supplement of O_2 to the Al_2O_3/AlN interface is therefore superior to the consumption of O_2 owing to oxidation of AlN. In other words, the interfacial oxidation rate is lower than the O_2 diffusion rate. And hence the former is actually the rate-controlling step in the oxidation process of the AlN substrates.

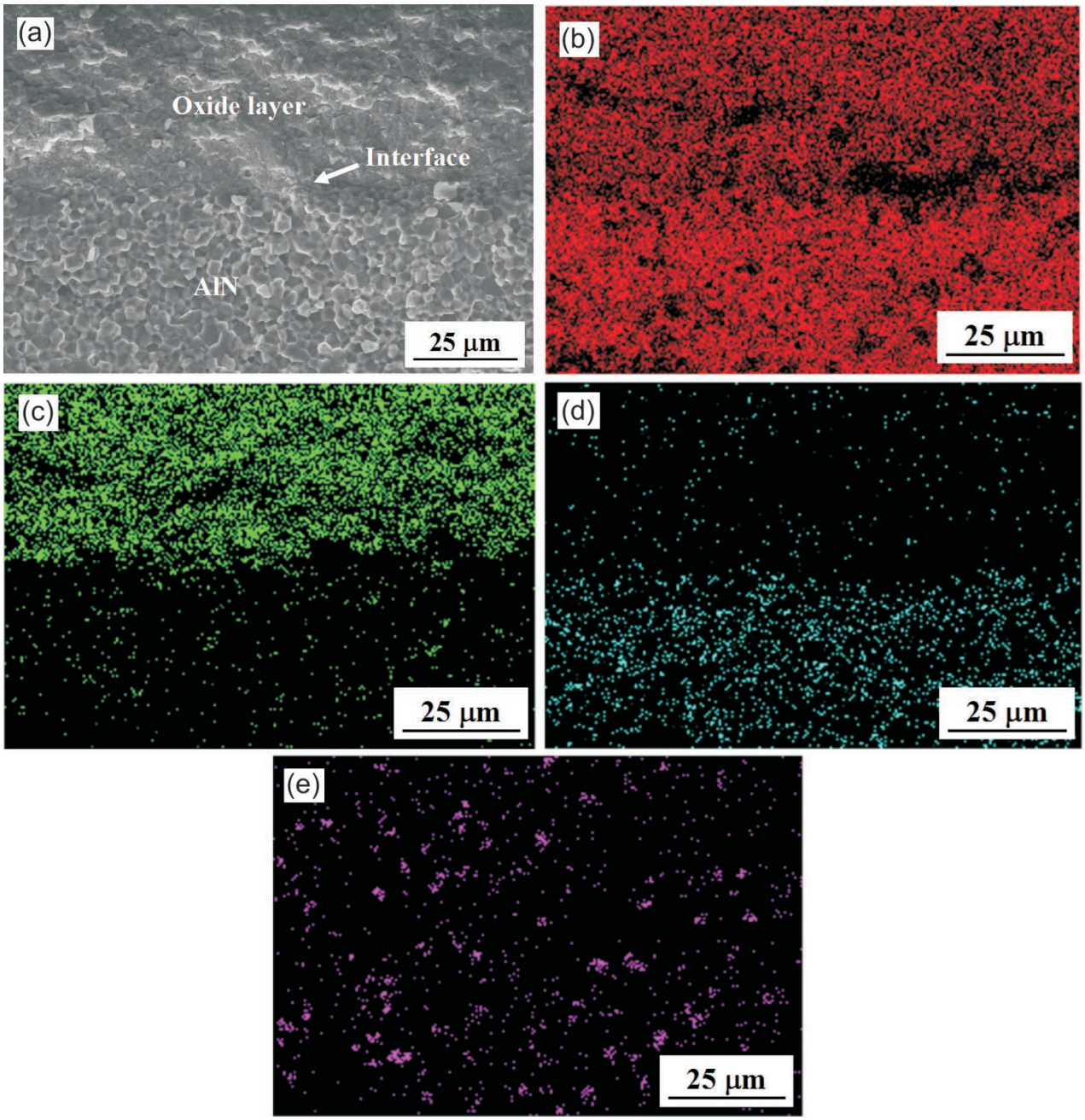

Fig. 2: SEM image and EDS elemental scanning mappings of the fracture surface of the AlN substrate oxidized at 1200 °C for 250 min (a) SEM image; (b) Element Al; (c) Element O; (d) Element N; (e) Element Y.

Generally, the solid-phase reaction rate constant (k) is a function of the reaction temperature (T), according to the Arrhenius equation:

$$k = k_0 \exp\left\{\frac{-E_a}{RT}\right\} \quad (1)$$

where k_0 is the pre-exponential factor, E_a is the activation energy, R is the general gas constant and T is the absolute temperature, respectively. In Fig. 7, a linear relationship of the natural logarithm of the oxidation rate constant ($\ln k$) and the reciprocal of the oxidation temperature ($1/T$) was plotted, and the oxidation activation energy of the AlN substrate was then derived (260.5 kJ mol^{-1}). The value is close to the linear oxidation activation energy of the AlN ceramics doped with 2 wt% Sm_2O_3 and 3 wt% Dy_2O_3 (243.9 kJ mol^{-1}) [26], although the sintering additives in these are different.

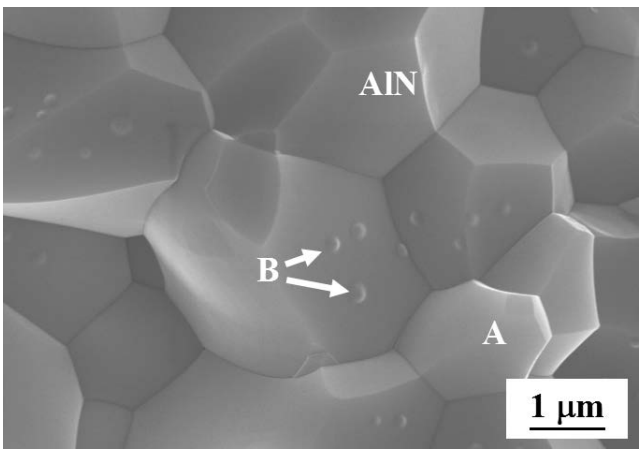

Fig. 3: SEM image showing the distributions of the YAG phase in the AlN ceramics.

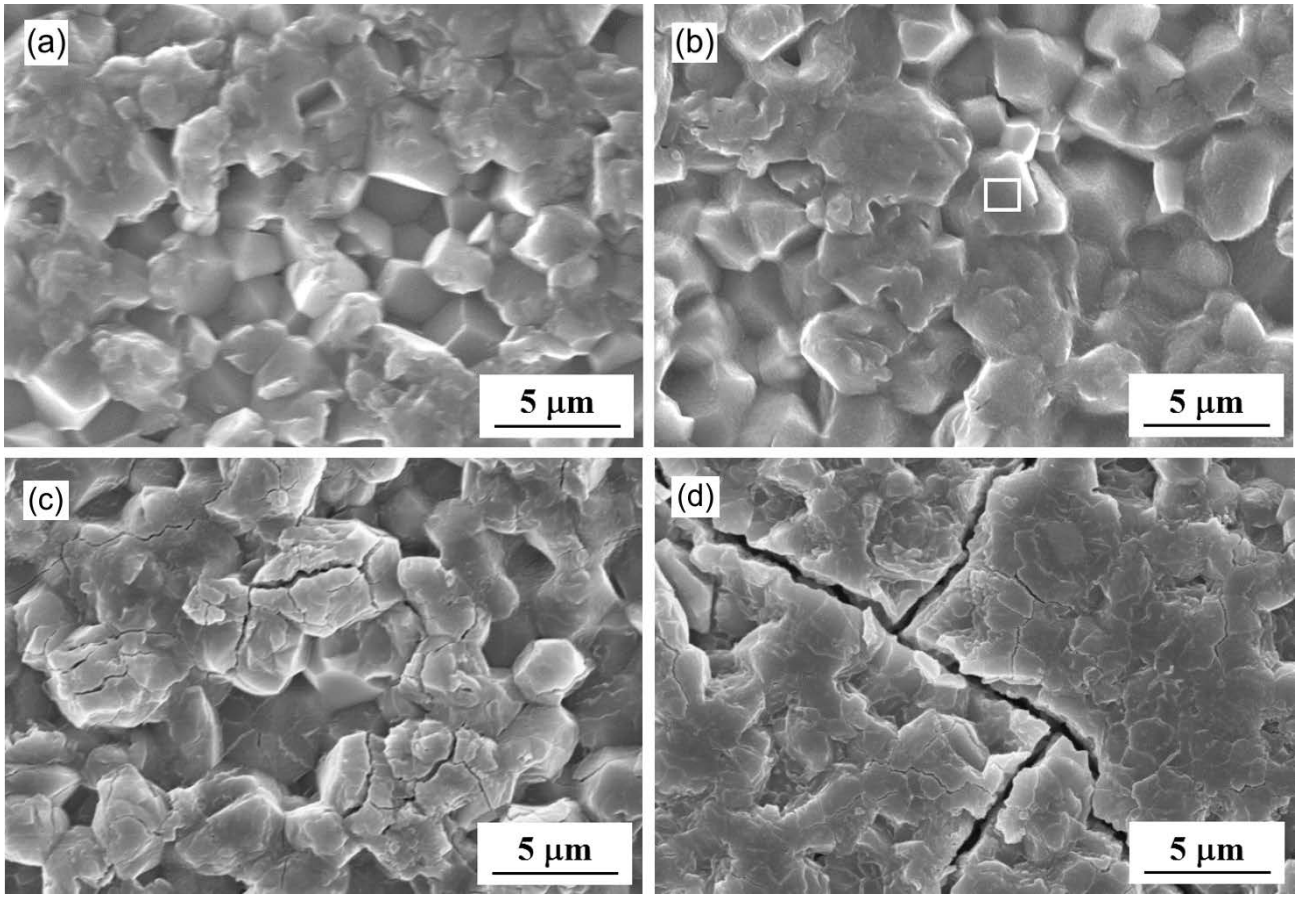

Fig. 4: Planar SEM images of the AlN substrates oxidized at different temperatures for various times (a) As-received; (b) 1000 °C for 150 min; (c) 1100 °C for 150 min; (d) 1200 °C for 100 min.

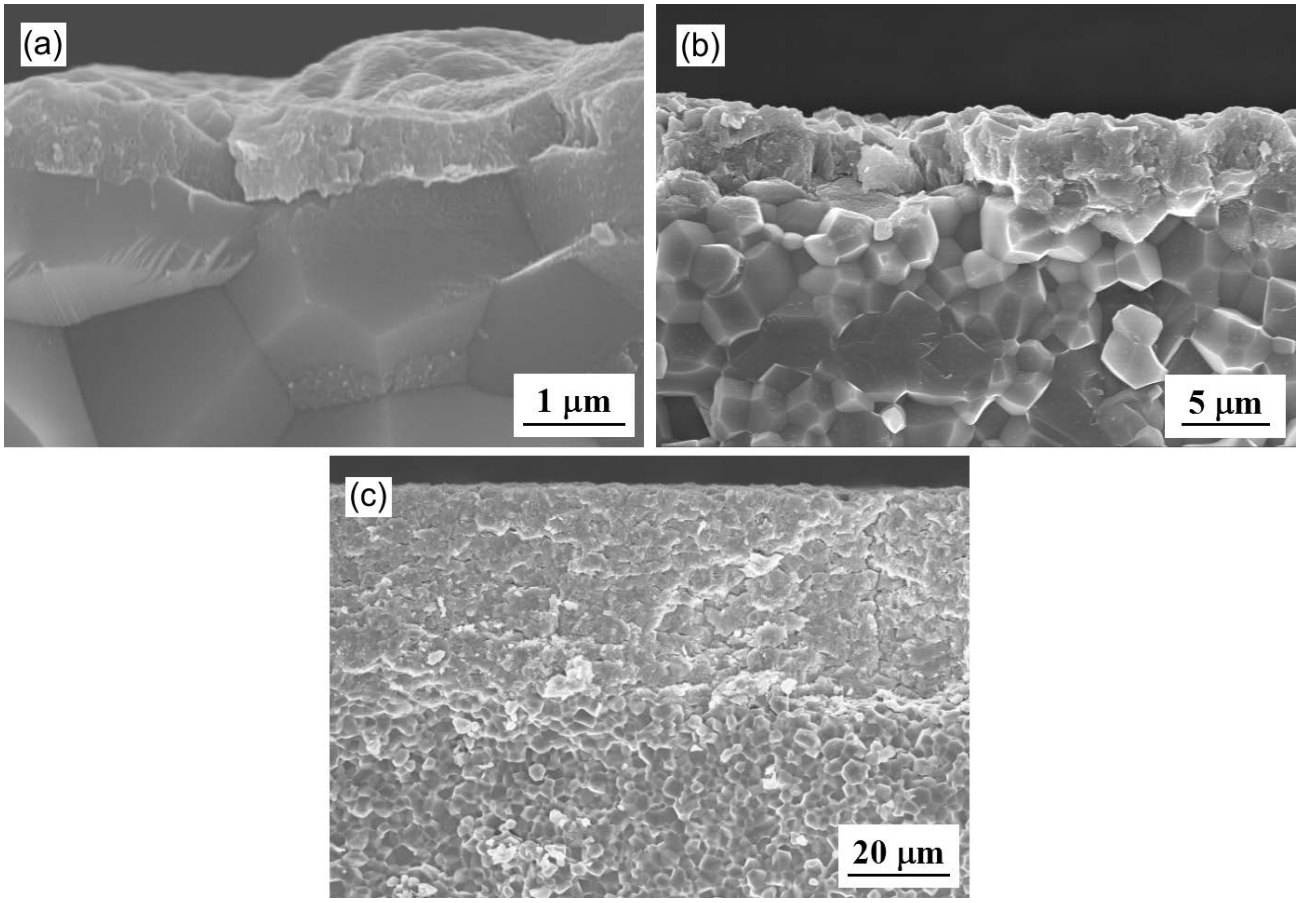

Fig. 5: SEM fractographs of the AlN substrates oxidized at different temperatures for 150 min (a) 1000 °C; (b) 1100 °C; (c) 1200 °C.

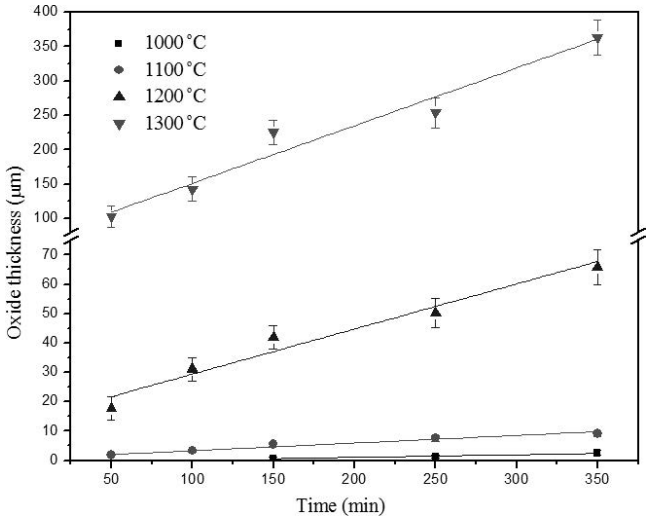

Fig. 6: Relationships of the thicknesses of the oxide layers vs. time as the AlN substrates oxidized at different temperatures.

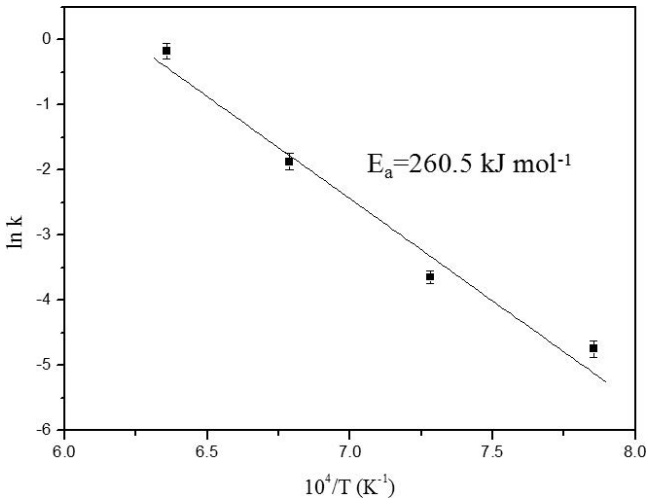

Fig. 7: Arrhenius plot of the oxide rate constants of the AlN substrates vs. the oxidation temperature.

(3) Formation mechanism

As shown by an arrow in Fig. 8a, the AlN triple grain boundary acts as the main O_2 transportation path. Different surfaces of the AlN grain in Fig. 8a are in different oxidation states: GB1, the farthest from the AlN triple grain boundary, is not yet undergoing oxidation. However, oxidation of GB2 and GB3 is apparently already happening at this time. The Al_2O_3 grains on GB2 decrease from 100 nm to 10 nm in size along the O_2 diffusing orientation. They eventually connect with each other to form a continuous, multi-pore Al_2O_3 layer. A magnification image in Fig. 8b shows the more detailed appearance of the multi-pore Al_2O_3 layer, which contains lots of nanotubes in the direction perpendicular to GB3. Chen reported a similar nano-pore microstructure of nanocrystalline Al_2O_3 ceramics [27]. Therefore, the pores in the oxide layer are also related to the formation and growth of the Al_2O_3 nano-grains, besides the N_2 release during the oxidation process.

The AlN grain boundary provides a fast diffusion path during oxidation of the AlN substrate. The oxidation process originates from the AlN grain boundaries and then extends into the AlN grains to form a core-shell structure, i.e. the inner AlN core is wrapped in a continuous Al_2O_3 shell layer (Fig. 9a). However, the separation along the core/shell interface indicates a weak core/shell interface bonding (Fig. 9b). Similarly, the interface bonding between two adjacent Al_2O_3 shells is also weak, resulting in the formation of interface micro-cracks, as indicated by an arrow in Fig. 9b.

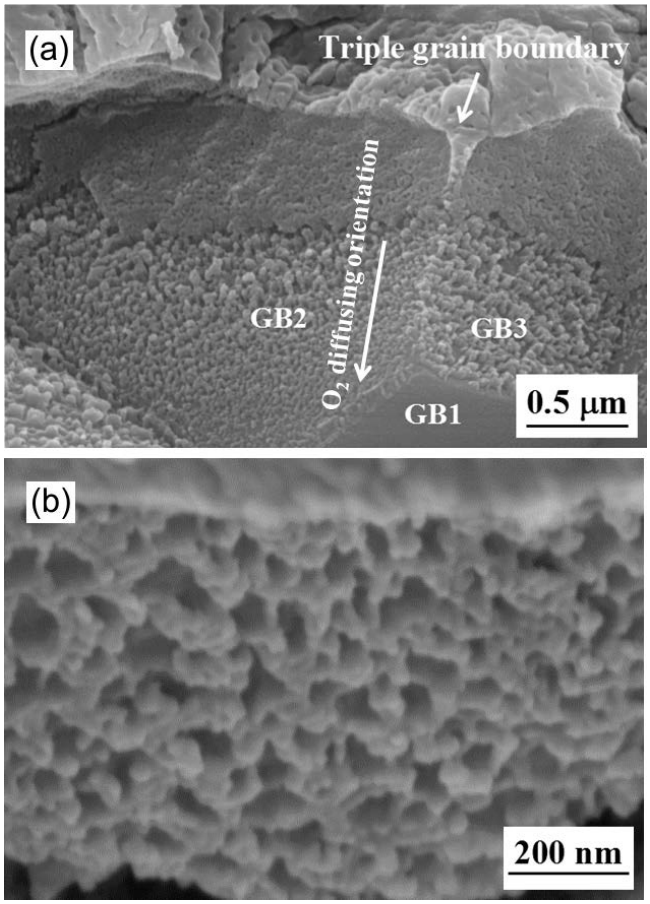

Fig. 8: SEM micrographs showing the initial oxidation of the AlN grain (a) 1100 °C for 350 min; (b) High magnification of GB3 in Fig. a.

The continuous pores along the Al_2O_3 grain boundaries construct the main paths of O_2/N_2 input/output in the oxide layer, as shown by the arrows in Fig. 10a. In the oxidized AlN substrate, the previously existing AlN grains have completely transformed into Al_2O_3 grain clusters. Flat pores exist between two neighboring Al_2O_3 grain clusters, as shown by an arrow in Fig. 10b, acting as the O_2/N_2 input/output channels between the main paths to the AlN reaction interface. These flat pores have likely coalesced to form the transverse cracks under the residual stress in the oxide layer (Fig. 5e). A nanotube structure of the pores near the AlN reaction interface is shown more clearly by the arrows in Fig. 10c. These pores are the final/initial segment of the O_2/N_2 input/output from the oxide layer to the AlN reaction interface.

During the oxidation process, the α-Al_2O_3 nano grains grow spontaneously and continuously, resulting in elimination of the pores and full densification of the

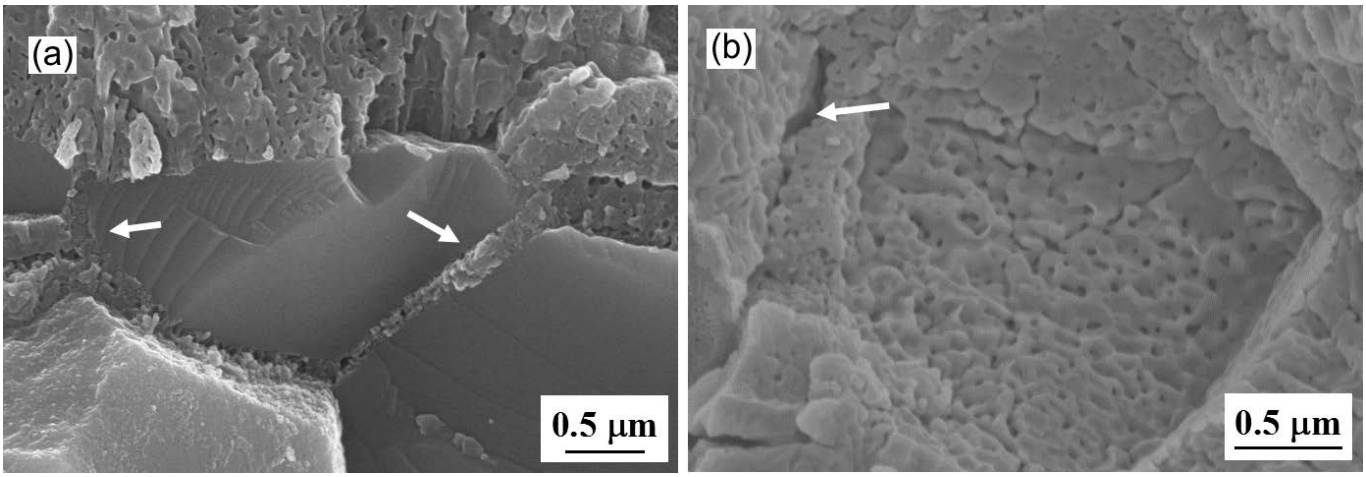

Fig. 9: SEM fractographs of the oxidized AlN substrates (a) 1100 °C for 50 min; (b) 1300 °C for 350 min.

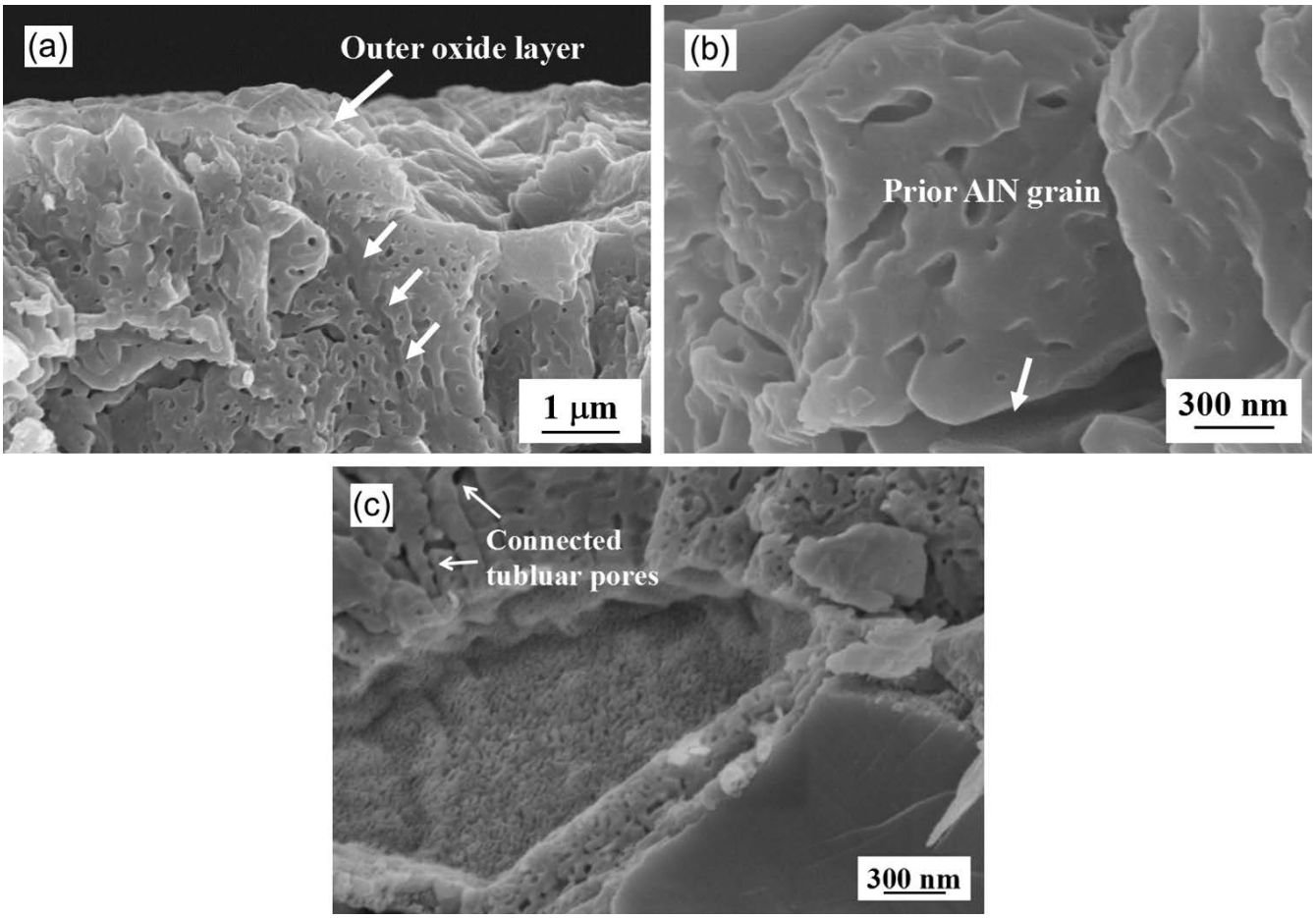

Fig. 10: SEM images of the fracture surfaces of the AlN substrates oxidized at 1200 °C for 100 min (a) The oxide layer; (b) High-magnification image of Fig. a showing the Al_2O_3 cluster; (c) High-magnification image of Fig. a showing the oxide layer connected to the AlN oxidation interface.

outermost oxide layer (Fig. 10a). Once a continuous and dense oxide layer is formed, the O_2/N_2 input/output paths are obstructed. Accordingly, O_2 diffusion in the oxide layer becomes the rate-controlled step in oxidation of the AlN substrate. Microstructure investigation in this work firstly gives an explicit explanation for the common view, i.e. the oxidation of AlN ceramics mostly follows a linear mechanism at 1000 – 1300 °C, but a parabolic one at 1350 °C and above, as reported in Refs. 13 and 24.

On the basis of the above research, a model concerning the microstructure and formation mechanism of the oxide layer has therefore been established (Fig. 11). During oxidation of the AlN substrate, O_2 diffuses along the AlN grain boundaries into the AlN grains to construct a core-shell structure. The nanotube pores in the oxide shells connect with the main paths in the oxide layer to construct a continuous O_2/N_2 input/output channel. It guarantees that oxidation of the AlN substrate follows the reaction-rate-controlled mechanism.

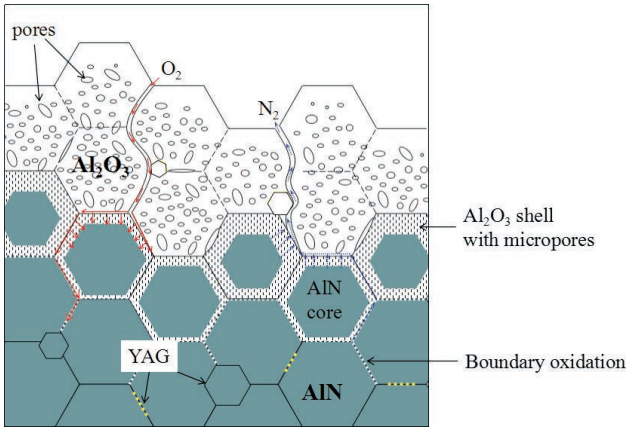

Fig. 11: A model of the oxidation of the AlN substrates.

IV. Conclusions

1) As the AlN substrates anneal at 1000 – 1300 °C in air, superficial cracks firstly form and then coalesce and propagate to form the longitudinal cracks in the oxide layer. The transverse cracks originate from the flat pores between the Al_2O_3 clusters and coalesce induced by the residual stress in the oxide layer.
2) The oxide layer growth is linearly related to the oxidation time with an activation energy of 260.5 kJ mol^{-1}, indicating reaction-rate-controlled kinetics. The Al_2O_3 nano-grains initially generate at the AlN grain boundaries, and then grow perpendicularly to the AlN grain boundaries to form a continuous oxide layer with nanotube pores. The formation of the pores results from the output of N_2 during the AlN oxidation and also the growth of the Al_2O_3 nano-grains.
3) Oxidation of the AlN substrates originates from the AlN grain boundaries broadened by YAG secondary grains. A core-shell structure composed of the AlN core wrapped in the continuous Al_2O_3 shell layer is then formed. Bonding at the core/shell interface and between two neighboring Al_2O_3 shells is weak.
4) In the oxide layer, the connected pores construct a continuous fast path for the O_2/N_2 input/output. As a result, the reaction-rate-controlled kinetic mechanism is followed. A model concerning the microstructure and mechanism for the formation of the oxide layer on the AlN substrates has been established.

Acknowledgements

This work was financially supported by Projects of Scientific and Technological Research, Anhui Province, China (Grant Nos. 15czz02047, 1604a0902162).

References

1 Khor, K.A., Yu, L.G., Murakoshi Y.: Spark plasma sintering of Sm_2O_3-doped aluminum nitride, *J. Eur. Ceram. Soc.*, **25**, 1057 – 1065, (2005).

2 Schulz-Harder, J.: Advantages and new development of direct bonded copper substrates, *Microelectron. Reliab.*, **43**, 359 – 365, (2003).

3 He, H., Fu, R., Wang, D., Song, X., Jing, M.: A new method for preparation of direct bonding copper substrate on Al_2O_3, *Mater. Lett.*, **61**, 4131 – 4133, (2007).

4 Yim, W.M., Paff R.J.: Thermal expansion of AlN, sapphire, and silicon, *J. Appl. Phys.*, **45**, 1456 – 1457, (1974).

5 Zhan, J., Cao, Y., Zhang, H., Guo, J., Zhang, J.H., Geng, C.L., Shi, C.D., Cui, S., Tang, W.M.: Low-temperature sintering of AlN ceramics by Sm_2O_3-Y_2O_3-CaO sintering additives formed via decomposition of nitrate solutions, *J. Mater. Eng. Perform.*, **26**, 1 – 7, (2017).

6 Zhan, J., Wu, Y.B., Zhang, H., Liu, J.Y., Guo, J., Geng, C.L., Cui, S., Tang, W.M.: Secondary phases, microstructures and properties of AlN ceramics sintered by adding nitrate sintering additives, *Adv. Appl. Ceram.*, **114**, 77 – 81, (2015).

7 Baik, Y.R., Drew, A.L.: Aluminum nitride: Processing and applications, *Key Eng. Mater.*, **122 – 124**, 553 – 570, (1996).

8 Haibo, J., Chen, K., Heping, Z., Agathopoulos, S., Fabrichnaya, O., Ferreira, J.M.F.: Direct nitridation of molten Al(Mg, Si) alloy to AlN, *J. Cryst. Growth.*, **281**, 639 – 645, (2005).

9 Iwase, N., Anzai, K., Shinozaki, K., Hirao, O., Thanh, T. D., Sugiura, Y.: Thick film and direct bond copper forming technologies for aluminum nitride substrate, *IEEE Trans. Compon. Hybrids Manuf. Technol.*, **8**, 253 – 258, (2003).

10 Barlak, M., Olesińska, W., Piekoszewski, J., Chmielewski, M., Jagielski, J., Kaliński, D., Werner, Z., Sartowska, B.: Ion implantation as a pre-treatment method of AlN substrate for direct bonding with copper, *Vacuum*, **78**, 205 – 209, (2005).

11 Jarrige, J., Joyeux, T., Lecompte, J.P., Labbe, J.C.: Influence of oxygen on the joining between copper and aluminium nitride, *J. Eur. Ceram. Soc.*, **27**, 337 – 341, (2007).

12 Tuan, W.H., Lee, S.K.: Eutectic bonding of copper to ceramics for thermal dissipation applications – a review, *J. Eur. Ceram. Soc.*, **34**, 4117 – 4130, (2014).

13 Osborne, E.W., Norton, M.G.: Oxidation of aluminum nitride, *J. Mater. Sci.*, **33**, 3859 – 3865, (1999).

14 Bellosi, A., Landi, E., Tampieri, A.: Oxidation behavior of aluminum nitride, *J. Mater. Res.*, **8**, 565 – 572, (1993).

15 Yeh, C.T., Tuan, W.H.: Oxidation mechanism of aluminum nitride revisited, *J. Adv. Ceram.*, **6**, 27 – 32, (2017).

16 Lavrenko, V. A., Alexeev, A.F.: Oxidation of sintered aluminum nitride, *Ceram. Int.*, **9**, 80 – 82, (1983).

17 Sato, T., Haryu, K., Endo, T., Shimada, M.: High temperature oxidation of hot-pressed aluminum nitride by water vapor, *J. Mater. Sci.*, **22**, 2277 – 2280, (1987).

18 Xu, X.R., Yan, W. L., Zhuang H.R., Li, W.L., Xu, S.Y.: Oxidation behavior of aluminum nitride, *J. Inorg. Mater.*, **18**, 337 – 342, (2003).

19 Kim, H.E., Moorhead, A.J.: Oxidation behavior and flexural strength of aluminum nitride exposed to air at elevated temperatures, *J. Am. Ceram. Soc.*, **77**, 1037 – 1041, (1994).

20 Katnani, A.D., Papathomas K.I.: Kinetics and initial stages of oxidation of aluminum nitride: thermogravimetric analysis and X-ray photoelectron spectroscopy study, *J. Vac. Sci. Technol. A.*, **5**, 1335 – 1340, (1987).

21 Suryanarayana, D.: Oxidation kinetics of aluminum nitride, *J. Am. Ceram. Soc.*, **73**, 1108 – 1110, (1990).

22 Zhou, H., Qiao, L., Fu, R.: Effect of the fluoride additives on the oxidation of AlN, *Mater. Res. Bull.*, **37**, 2427 – 2435, (2002).

23 Robinson, D., Dieckmann, R.: Oxidation of aluminum nitride substrates, *J. Mater. Sci.*, **29**, 1949 – 1957, (1994).

24 Tseng, W.J., Tsai, C.J., Fu, S.L.: Oxidation, microstructure and metallization of aluminum nitride substrates, *J. Mater. Sci.-Mater. Electron.*, **11**, 131 – 138, (2000).

25 Xiong, Y., Wang, H., Fu, Z.: Transient liquid-phase sintering of AlN ceramics with CaF_2 additive, *J. Eur. Ceram. Soc.*, **33**, 2199 – 2205, (2013).

26 Hou, X.M., Chou, K.C.: Quantitative interpretation of the parabolic and nonparabolic oxidation behavior of nitride ceramic, *J. Eur. Ceram. Soc.*, **29**, 517 – 523, (2009).

27 Chen, W.: Study on microstructure evolution and control of the α-Al_2O_3 growth, Doctoral Dissertation, Central South University, China, 2010.